

# Contact Binaries in OGLE-I Database\*

M. S z y m a ń s k i, M. K u b i a k and A. U d a l s k i  
 Warsaw University Observatory, Al. Ujazdowskie 4, 00-478 Warsaw, Poland  
 e-mail (msz,mk,udalski)@astrouw.edu.pl

## ABSTRACT

We present a new catalog of 1575 contact binary stars fainter than  $I = 18$  mag identified in OGLE-I database in the selected directions toward the Galactic bulge and the Galactic bar. For completeness we recall here also the objects from the formerly published OGLE catalog of contact binaries brighter than  $I = 18$  mag.

To ease the comparison and/or distinction between contact binaries with sinusoidal light curves and pulsating stars we also give a catalog of 506 objects with nearly sinusoidal light curves which were classified or re-classified as pulsating variable stars.

Present catalog contains the most numerous, observationally homogeneous sample of contact binaries. Given are the statistical properties of the sample relating to the distributions of brightness, periods and amplitudes of the contact binaries.

## 1 Introduction

The Optical Gravitational Lensing Experiment (OGLE) is a long term project of searching for the dark matter in the Universe with microlensing phenomena (Paczynski 1986, Udalski *et al.* 1993b). The first phase of the project (OGLE-I) started in 1992 and lasted over four consecutive observing seasons till 1995. The 1-m Swope telescope at the Las Campanas Observatory in Chile, operated by the Carnegie Institution of Washington, was used for observations. During the entire program the detector was a  $2048 \times 2048$  Ford/Loral CCD camera. Its pixel size,  $15 \mu\text{m}$ , corresponded to the image scale of 0.44 arcsec/pixel – sufficient for resolving stars in dense fields. Eighteen fields  $15 \times 15$  arcmin were monitored during a period spanning more than 1200 days providing more than 240 observations of each field through filter  $I$ . Each field was also observed, although less frequently (20–30 times), through filter  $V$ . The coordinates of the centers of the fields are given in Table 1. Fields with names beginning with the letters “BW” are located in the Baade’s window and those beginning with the letters “MM” – in the Galactic bar. The last column of Table 1 gives the total number of stars distinguished on the  $I$ -band template image of each field.

Observations were reduced practically on-line with the procedure described in detail in Udalski *et al.* (1992) and the results were collected in a database as described by Szymański and Udalski (1993a). Udalski *et al.* (1992) also gave a detailed analysis of photometric errors. It will be sufficient to recall here that the errors of single observation depend on brightness and vary from about 0.015–0.020 mag (depending on the image quality) at  $I=14.5$  mag to about 0.08–0.13 mag at  $I = 18.5$  mag. Unfortunately the magnitude scale is somewhat non-linear due to non-linearity of the CCD detector used. While the accuracy of standard system magnitudes is about  $\pm 0.04$  mag for the brighter stars, it drops to about  $\pm 0.10$  mag at the faint end.

One of the “by-products” of the OGLE-I observations was the Catalog of Periodic Variable Stars in the Galactic bulge published in a series of papers by Udalski *et al.* (1994, 1995a,b, 1996, 1997). Due to a large number of observed stars the Catalog was limited to objects brighter than  $I = 18.0$  mag. The upper limit of brightness,  $I \approx 14$  mag, resulted from saturation of bright star images on the CCD detector.

## 2 Contact Binaries in the OGLE-I Database

The already published Catalog of Periodic Variable Stars in the Galactic bulge lists, among others, 1166 objects classified as contact binaries (EW). The only criterion of classification was the shape of their light curves. In the case of relatively bright stars for which observational errors are small and the definition of the light curve is good, this was enough for unambiguous classification.

---

\*Based on observations obtained at the Las Campanas Observatory of the Carnegie Institution of Washington.

Table 1  
OGLE-I Fields

Field	RA (2000.0)	DEC (2000.0)	$l$	$b$	Number of stars on a template
BW1	18 <sup>h</sup> 02 <sup>m</sup> 24 <sup>s</sup>	−29°49′05″	1°1	−3°6	207251
BW2	18 <sup>h</sup> 02 <sup>m</sup> 24 <sup>s</sup>	−30°15′05″	0°7	−3°8	234443
BW3	18 <sup>h</sup> 04 <sup>m</sup> 24 <sup>s</sup>	−30°15′05″	0°9	−4°2	174349
BW4	18 <sup>h</sup> 04 <sup>m</sup> 24 <sup>s</sup>	−29°49′05″	1°3	−4°0	234258
BW5	18 <sup>h</sup> 02 <sup>m</sup> 24 <sup>s</sup>	−30°02′05″	0°9	−3°7	197246
BW6	18 <sup>h</sup> 03 <sup>m</sup> 24 <sup>s</sup>	−30°15′05″	0°8	−4°0	226301
BW7	18 <sup>h</sup> 04 <sup>m</sup> 24 <sup>s</sup>	−30°02′05″	1°1	−4°1	193559
BW8	18 <sup>h</sup> 03 <sup>m</sup> 24 <sup>s</sup>	−29°49′05″	1°2	−3°8	233591
BW9	18 <sup>h</sup> 00 <sup>m</sup> 50 <sup>s</sup>	−29°49′05″	0°9	−3°3	265840
BW10	18 <sup>h</sup> 00 <sup>m</sup> 50 <sup>s</sup>	−50°02′05″	0°7	−3°4	255248
BW11	18 <sup>h</sup> 00 <sup>m</sup> 50 <sup>s</sup>	−30°15′05″	0°5	−3°5	250170
BWC	18 <sup>h</sup> 03 <sup>m</sup> 24 <sup>s</sup>	−30°02′00″	1°0	−3°9	254481
MM1-A	18 <sup>h</sup> 06 <sup>m</sup> 52 <sup>s</sup>	−26°38′05″	4°4	−2°9	242602
MM1-B	18 <sup>h</sup> 06 <sup>m</sup> 52 <sup>s</sup>	−26°51′05″	4°2	−3°0	247554
MM5-A	17 <sup>h</sup> 47 <sup>m</sup> 30 <sup>s</sup>	−34°45′00″	−4°8	−3°4	231279
MM5-B	17 <sup>h</sup> 47 <sup>m</sup> 30 <sup>s</sup>	−34°57′00″	−4°9	−3°5	175449
MM7-A	18 <sup>h</sup> 10 <sup>m</sup> 53 <sup>s</sup>	−25°54′20″	5°4	−3°3	221018
MM7-B	18 <sup>h</sup> 11 <sup>m</sup> 47 <sup>s</sup>	−25°54′20″	5°5	−3°5	160630

We extended the search for variable stars to the objects with  $I$  brightness between 18 and about 19.5 mag. Stars searched for variability were extracted from the  $I$ -band database in the same way as in the former Catalog, *i.e.*, the star should have at least 40 good observations (typically 100–200 observations) and the standard deviation of the magnitude had to be larger than the sigma limit for non-variable stars of a given magnitude (Udalski *et al.* 1993a). The selected objects were subject to period search procedure both with the classic periodogram analysis and with the phase dispersion minimization method of Stellingwerf (1978). About two thousand new objects with periodic light variations were found. The majority of them had light curves typical for contact binaries and their identification was straightforward. The well known problem, however, posed the distinguishing between sinusoidal pulsators and contact binaries with sinusoidal shape of light curve and two times longer periods. Although this distinction may be very difficult in particular cases it can be done in a statistical sense.

To show this we used for quantitative description of the light curves the Fourier decomposition method in which the observed light variations  $A(t)$ , with a period  $P = 2\pi/\omega$  known from periodogram analysis, are approximated by the sum of harmonics

$$A(t) = a_0 + \sum_i a_i \cos(i \cdot \omega t + f_i) \quad (1)$$

We performed these calculations up to the fifth harmonic for all objects with periodic light variations, adopting such values of periods that the light curves showed two minima in one cycle, *i.e.*, we treated all variable stars as EW-type objects. From them we selected two groups of about four hundred objects each: evident pulsators *i.e.*, objects with periods shorter than about 0.2 d and/or with shapes of light curves that could not be mistaken with EW-type variable stars and evident W UMa objects (randomly selected bright objects with well defined EW-type light curves). The relations between phases  $f_2$  and  $f_4$  for both groups are shown in Fig. 1. It can easily be seen that there exists a well defined relation between these two phases for contact binaries, whereas the same relations for pulsating variable stars is very weak. Using this result in doubtful cases, when the unambiguous identification of the light curve was not obvious, the objects fulfilling the relation for contact binaries were classified as EW and the objects laying off this relation – as pulsating variables P. We believe that this procedure (applied to less than 10% of all objects with equal depths of minima which appeared to be "doubtful") reduces the expected number of misidentifications in our samples of EW and pulsating variable stars down to about one percent.

One of the easily recognized features of the contact binary type light curve is the relative depth of eclipses. By visual inspection we divided our sample of EW variable stars into two groups: "EWa" with markedly different depths of minima, and "EWs" – for which, within the error limits, the depths of

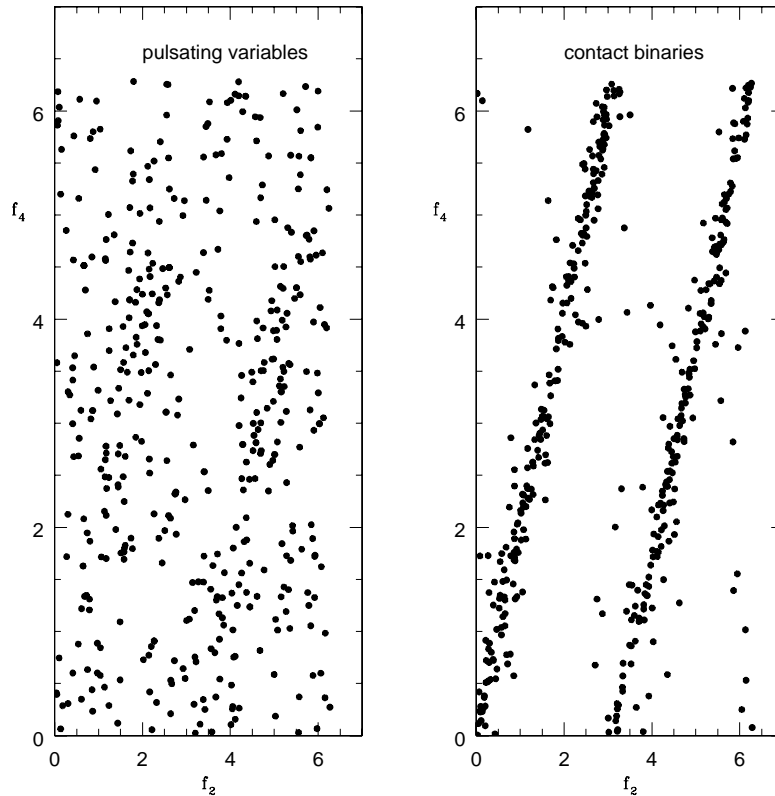


Fig. 1. Relation between phase constants  $f_2$  and  $f_4$  (from Eq. 1) for pulsating stars (left panel) and contact binaries (right panel). The relation between  $f_2$  and  $f_4$  in the right panel is equivalent to  $f_2 - 2f_4 = 0$ . Phases are expressed in radians.

both minima are the same. The two groups are statistically and probably also physically nonequivalent. The EWs group contains objects with the same or very close surface temperature of the components, whereas the different depths of eclipses suggest different temperatures. On the other hand, the sample of stars with different depths of minima is more uniform in the sense that it is not contaminated with single pulsating stars: contact binaries with different depths of minima can hardly be mistaken with pulsating variable stars.

### 3 The Catalog

The catalog of contact binaries can be found in anonymous FTP archive at

[ftp://ftp.astroww.edu.pl/ogle/ogle1/contact\\_binaries](ftp://ftp.astroww.edu.pl/ogle/ogle1/contact_binaries)

or on its US mirror at

[ftp://bulge.princeton.edu/ogle/ogle1/contact\\_binaries](ftp://bulge.princeton.edu/ogle/ogle1/contact_binaries)

The newly found W UMa variable stars are listed in tables named EWa.new (595 entries) and EWs.new (980 entries). For completeness, in tables EWa.old (525 entries) and EWs.old (641 entries), we repeat here the contact binaries from the already published Catalog of OGLE-I variable stars. The consecutive columns of these tables contain: (1) – name of the OGLE-I field, (2) – number of the object in OGLE-I database (3) – Right Ascension (2000.0), (4) – Declination (2000.0), (5) – observed mean magnitude in filter  $I$ , (6) – observed  $V - I$  (9.99 means lack of  $V - I$  measurements), (7) – period in days, (8) – character of the light curve. The objects are ordered according to the increasing values of periods. For illustration, the beginning of the table EWa.new is reproduced here in Table 2.

The archive contains also results of photometric observations of the stars from the catalog and finding charts. Please see README file there for detailed description of the archive contents.

Table 2

A sample page from the the table “EWa.new” containing newly identified contact binaries in OGLE-I database.

Field	No	RA(2000.0)	DEC(2000.0)	$I$ [mag]	$V - I$ [mag]	Period [d]	Type
BW9	189794	18 <sup>h</sup> 00 <sup>m</sup> 49 <sup>s</sup> 45	-29°41'53''6	18.83	2.22	.20680	EWa
MM1-A	128388	18 <sup>h</sup> 06 <sup>m</sup> 52 <sup>s</sup> 74	-26°35'41''6	18.98	1.60	.23516	EWa
BW5	166779	18 <sup>h</sup> 02 <sup>m</sup> 35 <sup>s</sup> 99	-29°55'37''1	18.58	9.99	.23919	EWa
MM1-A	113202	18 <sup>h</sup> 06 <sup>m</sup> 48 <sup>s</sup> 63	-26°42'03''4	18.05	2.02	.24168	EWa
MM1-B	163429	18 <sup>h</sup> 06 <sup>m</sup> 54 <sup>s</sup> 64	-26°49'18''9	18.42	1.77	.24442	EWa
MM1-A	11980	18 <sup>h</sup> 06 <sup>m</sup> 18 <sup>s</sup> 58	-26°39'47''4	18.12	1.78	.25362	EWa
BW3	168639	18 <sup>h</sup> 04 <sup>m</sup> 45 <sup>s</sup> 11	-30°11'40''5	18.18	1.91	.25980	EWa
BW10	3060	18 <sup>h</sup> 00 <sup>m</sup> 18 <sup>s</sup> 98	-30°07'52''9	18.53	1.66	.26218	EWa
MM1-B	28221	18 <sup>h</sup> 06 <sup>m</sup> 15 <sup>s</sup> 34	-26°45'39''9	17.63	1.86	.26446	EWa
BW8	70608	18 <sup>h</sup> 03 <sup>m</sup> 07 <sup>s</sup> 78	-29°54'13''5	17.84	1.63	.26598	EWa
MM7-B	108382	18 <sup>h</sup> 11 <sup>m</sup> 50 <sup>s</sup> 75	-25°52'39''8	18.53	2.04	.26708	EWa
MM7-A	65167	18 <sup>h</sup> 10 <sup>m</sup> 43 <sup>s</sup> 67	-26°00'44''4	19.73	9.99	.26900	EWa
BW1	174918	18 <sup>h</sup> 02 <sup>m</sup> 37 <sup>s</sup> 68	-29°43'44''8	19.12	9.99	.26986	EWa
BW4	148730	18 <sup>h</sup> 04 <sup>m</sup> 26 <sup>s</sup> 32	-29°48'48''6	18.67	1.57	.27030	EWa
BW6	139978	18 <sup>h</sup> 03 <sup>m</sup> 29 <sup>s</sup> 76	-30°17'19''2	18.44	1.76	.27304	EWa
MM1-B	58328	18 <sup>h</sup> 06 <sup>m</sup> 33 <sup>s</sup> 60	-26°47'27''1	17.23	1.53	.27900	EWa
BW2	63876	18 <sup>h</sup> 02 <sup>m</sup> 09 <sup>s</sup> 37	-30°22'34''8	18.18	2.05	.28142	EWa
BW11	52517	18 <sup>h</sup> 00 <sup>m</sup> 24 <sup>s</sup> 28	-30°14'45''3	19.42	9.99	.28434	EWa
BW9	62576	18 <sup>h</sup> 00 <sup>m</sup> 28 <sup>s</sup> 34	-29°47'29''7	19.51	2.14	.28612	EWa
BW11	75418	18 <sup>h</sup> 00 <sup>m</sup> 39 <sup>s</sup> 94	-30°19'59''0	18.62	1.48	.28780	EWa
BW7	16970	18 <sup>h</sup> 03 <sup>m</sup> 53 <sup>s</sup> 37	-30°00'02''4	18.88	1.50	.28838	EWa
BW3	78973	18 <sup>h</sup> 04 <sup>m</sup> 23 <sup>s</sup> 74	-30°21'41''1	19.01	9.99	.28998	EWa
BW2	65073	18 <sup>h</sup> 02 <sup>m</sup> 08 <sup>s</sup> 60	-30°21'51''3	18.98	1.59	.29032	EWa
BW9	147608	18 <sup>h</sup> 00 <sup>m</sup> 43 <sup>s</sup> 74	-29°45'11''4	19.15	1.69	.29040	EWa
BW9	43248	18 <sup>h</sup> 00 <sup>m</sup> 27 <sup>s</sup> 40	-29°53'33''6	18.92	1.81	.29102	EWa
BW8	199379	18 <sup>h</sup> 03 <sup>m</sup> 37 <sup>s</sup> 68	-29°42'28''8	18.45	1.72	.29134	EWa
BW7	132331	18 <sup>h</sup> 04 <sup>m</sup> 26 <sup>s</sup> 34	-29°57'55''7	18.85	1.66	.29176	EWa
MM1-A	130188	18 <sup>h</sup> 06 <sup>m</sup> 45 <sup>s</sup> 13	-26°34'59''0	19.23	1.71	.29238	EWa
BW10	78472	18 <sup>h</sup> 00 <sup>m</sup> 36 <sup>s</sup> 63	-30°06'30''9	17.93	1.51	.29456	EWa
BWc	1362	18 <sup>h</sup> 02 <sup>m</sup> 51 <sup>s</sup> 58	-30°09'19''9	18.86	1.37	.29694	EWa
MM5-B	169652	17 <sup>h</sup> 47 <sup>m</sup> 48 <sup>s</sup> 61	-34°54'01''8	18.05	1.54	.29770	EWa
BW2	25180	18 <sup>h</sup> 01 <sup>m</sup> 52 <sup>s</sup> 88	-30°11'31''8	19.54	1.14	.29840	EWa
BWc	205530	18 <sup>h</sup> 03 <sup>m</sup> 38 <sup>s</sup> 37	-30°00'29''2	19.02	1.61	.29860	EWa
MM1-A	234696	18 <sup>h</sup> 07 <sup>m</sup> 12 <sup>s</sup> 70	-26°33'17''4	18.47	1.90	.29872	EWa
BW10	56593	18 <sup>h</sup> 00 <sup>m</sup> 28 <sup>s</sup> 33	-30°00'19''8	18.28	2.35	.29880	EWa
MM1-B	79232	18 <sup>h</sup> 06 <sup>m</sup> 36 <sup>s</sup> 89	-26°54'09''7	18.31	1.84	.29906	EWa
MM1-A	42504	18 <sup>h</sup> 06 <sup>m</sup> 35 <sup>s</sup> 91	-26°42'10''9	19.46	1.46	.29938	EWa
MM1-A	197164	18 <sup>h</sup> 07 <sup>m</sup> 10 <sup>s</sup> 15	-26°35'16''4	18.69	9.99	.30160	EWa
BW9	178667	18 <sup>h</sup> 00 <sup>m</sup> 52 <sup>s</sup> 53	-29°47'12''5	18.49	1.38	.30186	EWa
MM7-A	184242	18 <sup>h</sup> 11 <sup>m</sup> 06 <sup>s</sup> 08	-25°48'42''8	19.44	9.99	.30228	EWa
MM7-B	115327	18 <sup>h</sup> 11 <sup>m</sup> 45 <sup>s</sup> 80	-25°48'25''0	18.01	1.85	.30252	EWa
BW2	20210	18 <sup>h</sup> 01 <sup>m</sup> 50 <sup>s</sup> 69	-30°14'25''5	19.40	9.99	.30260	EWa

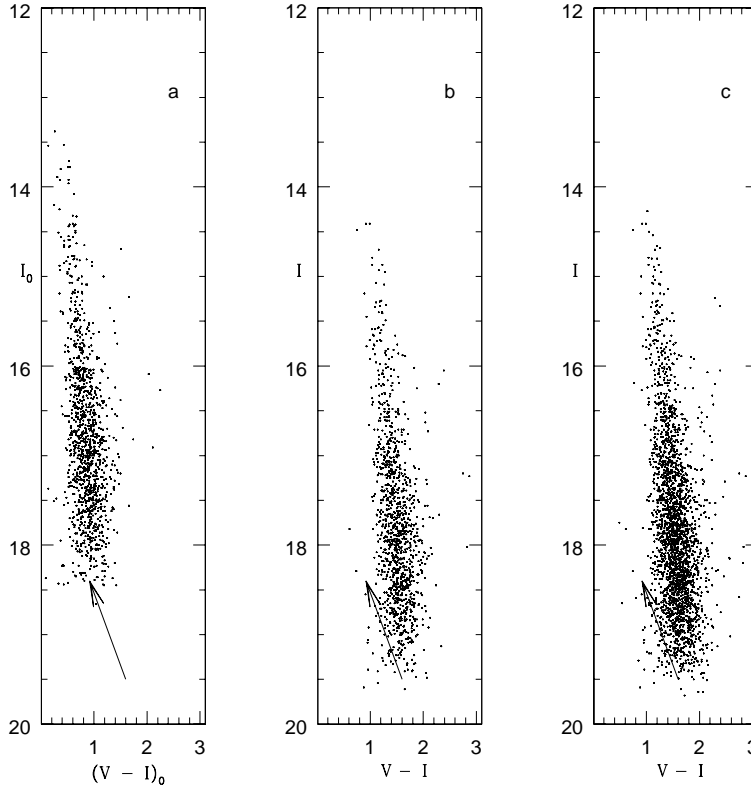


Fig. 2. Color – Brightness diagram for contact binaries. (a) – binaries corrected for interstellar extinction, (b) – the same stars not corrected for interstellar extinction. (c) – all binaries from our catalog. The arrow shows the average shift of both diagrams resulting from the absorption  $A_I = 1.1$  mag and  $E(V - I) = 0.68$  mag.

## 4 Color – Brightness Diagram and Brightness Distribution of the Galactic Bulge Contact Binaries

Objects in our database are subject to interstellar extinction and reddening. Woźniak and Stanek (1996) proposed an original method to investigate interstellar extinction based on two band photometry of the red clump stars. The method was applied by Stanek (1996) to the Baade’s window in which the red clump stars are very abundant. He constructed an extinction map covering large part of the OGLE-I fields. We used this map to apply the extinction corrections to the observed  $I$  and  $V - I$  for the total of 1277 (new and old) objects located in the central part of Baade’s window, covered by the Stanek’s extinction map. The extinction-corrected color–magnitude diagram for these objects is given in panel (a) of Fig. 2. Panel (b) shows this relation for the same stars not corrected for extinction. Relation for all observed stars, not corrected for interstellar extinction and reddening, is shown in panel (c). All diagrams are very similar; only the scatter of points in panel (a) is slightly smaller than in panel (b), suggesting that the applied extinction correction is physical and we are dealing, in major part at least, with objects located at the Galactic bulge distance. Were this not true then the application of the bulge value of extinction to our stars would be meaningless. In any case we may state that the interstellar extinction does not influence markedly the statistical relation between colors and magnitudes of stars in our sample. This relation seems to be determined by the true relation for double stars, by the interstellar extinction, and the observational errors. Please also note that the relation in Fig. 2 differs from the “main sequence” in the CMD diagrams given by Udalski *et al.* (1993a) for all stars observed in the direction of the Baade’s window and usually connected with the Galactic disk stars.

The distribution of the observed  $I$ -band brightness of the contact binaries from the present catalog is shown in Fig. 3. In panel (a) we compare these distributions for EWa and EWs objects. Except for the small, but apparently real, shift of EWs distribution toward fainter stars, both histograms look very similar and do not differ from the distribution of brightness of all EW binaries shown by the histogram in panel (c). The dashed curve in panel (c) shows the observed brightness distribution of all stars identified in all fields in the Baade’s window. There are two reasons why these two distributions are different. Firstly, the brightness of a contact binary is greater than the brightness of similar single star,

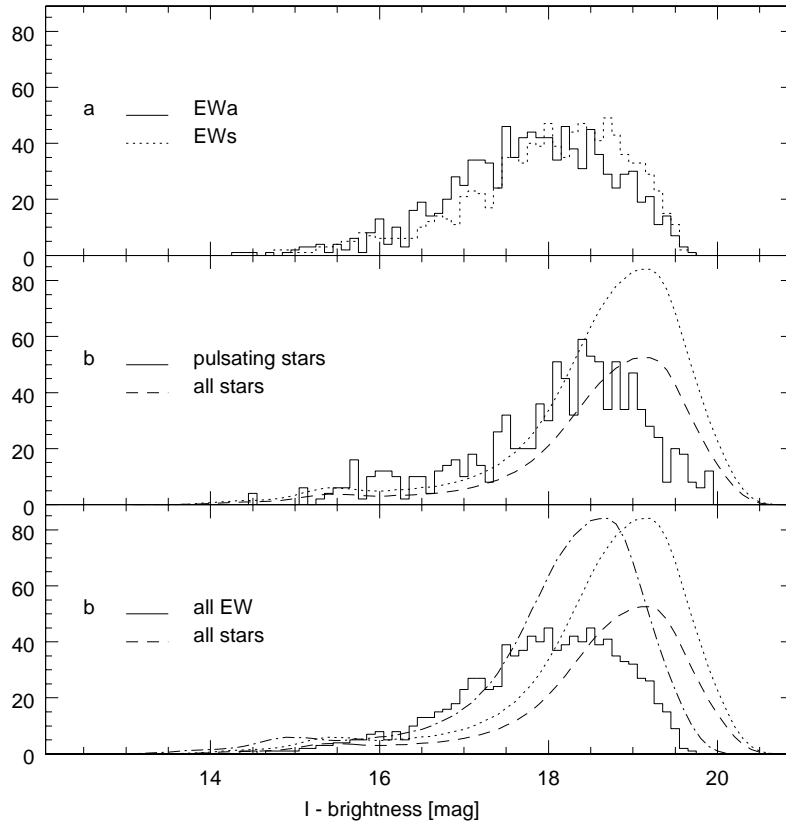


Fig. 3. Distribution of the observed  $I$ -band brightness of contact binaries from the present catalog: (a) – all EWa (1119) and all EWs (1621) binaries, not corrected for the interstellar extinction. (b) – histogram of brightness distribution of objects classified in our catalog as pulsating variables. Dashed line shows the brightness distribution of all stars identified in all fields in the direction of the Baade’s window. Dotted line is the latter distribution multiplied by 1.6 to give the best fit to the histogram. (c) – histogram of brightness distribution of all EW binaries compared with the distribution of brightness of all stars identified in all field in the direction of Baade’s window (dashed curve). Dashed-dotted curve shows the latter distribution multiplied by 1.6 and shifted by  $I$  scale by  $-0.5$  mag for the best fit with the histogram. The bin of the histograms is 0.1 mag; all distributions are normalized to 1000 objects.

and secondly, because both distributions are normalized to the same number of objects, the apparent lack of faint contact binaries due to all possible selection effects results in corresponding rise of relative number of brighter objects. To account in approximate way for this effects we show in panel (b) of Fig. 3 the observed brightness distribution of pulsating stars from our sample and compare it with the brightness distribution of all stars. Both distributions are different for the same reasons as above, except for the fact that the mean brightness of the single pulsating star is the same as the brightness of constant star with the same physical characteristics. We also assume – what may not be true – that the efficiency of discovery of bright pulsating stars is essentially the same as for constant stars. The latter was estimated by Udalski *et al.* (1993a). Their conclusion was that this quantity is approximately constant (although less than 1) over the range of magnitudes between 15 and 18 in  $I$  and diminishes rapidly for fainter stars.

If we accept the above assumption we may express the distributions from panel (b) of Fig. 3 as  $N_1 \cdot f_1(I)$  for constant stars and  $N_2 \cdot f_2(I)a(I)$  for pulsating stars.  $N_1$  and  $N_2$  are normalization factors, functions  $f_1(I)$  and  $f_2(I)$  describe true brightness distributions of all stars and pulsating stars, respectively; function  $a(I)$  describes the detection probability of pulsation in stars of a given  $I$ -band brightness (irrespective of the probability of identification of the object as a star, which is included in functions  $f(I)$ ).

If we assume additionally that pulsating stars are represented in the same proportion among the stars of all brightness, *i.e.*,  $f_1(I) = f_2(I)$ , and that for bright stars in  $I$ -band range 15–18 mag  $a(I) \approx 1$  then the distributions in this range are simply  $N_1 f(I)$  and  $N_2 f(I)$ , and with our assumptions should be the same. As it can be seen from panel (b) in Fig. 3 an acceptable agreement of both distributions for the stars brighter than about 18.5 mag can be obtained by multiplying the star brightness distribution by 1.6 (dotted line). It means that due to the influence of the “filter”  $a(I)$ , effective for the objects fainter than about 18 mag, the relative number of detected variable stars is reduced by a factor of  $1/1.6$ .

The comparison of the distribution multiplied by 1.6 (dotted line) with the histogram of brightness of contact binaries is shown in panel (c) of Fig. 3. The still remaining excess of contact binaries among bright stars is a result of their duplicity. Shift of about  $-0.5$  mag in the  $I$  scale seems to account for this effect (dashed-dotted line).

The fair agreement of the histogram with the dashed-dotted curve on their rising branches suggests that our efficiency of discovering variable stars in  $I$  brightness range 14–17.5 mag is the same as the efficiency of identifying constant stars and in this respect our sample is representative for the considered population of stars. The marked difference of both curves for fainter objects is a joint effect of the possible true difference in brightness distributions and the diminishing efficiency of variable star discovery. Separation of both effects does not seem to be possible. We can only draw a conclusion that the percentage of contact binary systems identified among the observed stars is smaller than the percentage of discovered pulsating stars and that the efficiency of discovering variable objects is not greater than about 60%.

## 5 Period Distribution

Period observations are practically free from selection effects that could affect directly the determined period value or the probability of the discovery of a variable object with a given period among the objects in a given range of brightness. The possible exception may be periods close to 0.5 day or 1 day, difficult to be determined observationally. In general, however, the period distribution is an important and observationally unbiased characteristic of a particular group of variable stars.

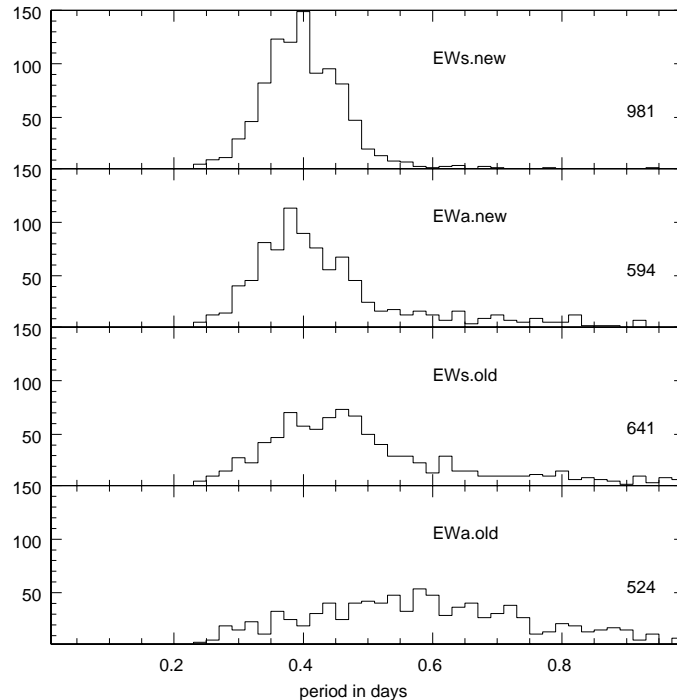


Fig. 4. Period distributions of the different groups of contact binaries in the present catalog. Period bins are 0.02 d wide. All distributions are normalized to 1000 objects; the real number of objects in each group is given in lower right corner of all panels.

Fig. 4 shows the period distributions for contact binaries from the OGLE Catalog of variable stars and for the newly discovered objects. Histograms represent numbers of objects within period bins of 0.02 day. All the distributions are normalized to the same number (1000) of objects. The distributions are markedly different and we think it could be instructive to present them in more detail.

Figs. 5 and 6 show period distributions for both groups of contact binaries (*i.e.*, with equal and unequal depths of minima) in different ranges of  $I$ -band brightness. It can be seen from Figs. 5 and 6 that the period distributions of EWa and EWs objects which are broad and different for stars brighter than  $I = 18$  mag become narrower and more similar for fainter stars. This reflects the character of the period – brightness relation (see below).

To check for the possible distortion of these distributions by misclassified pulsating stars we look

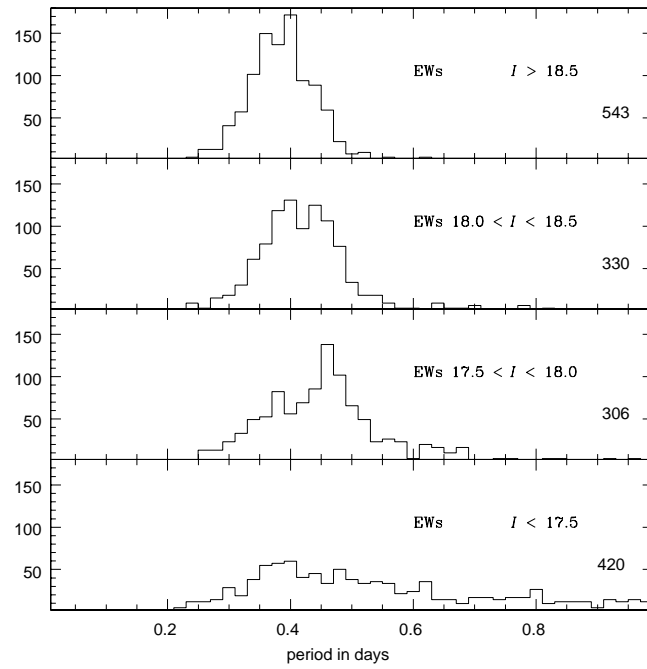


Fig. 5. Period distributions for contact binaries with equal depths of minima in different ranges of brightness.

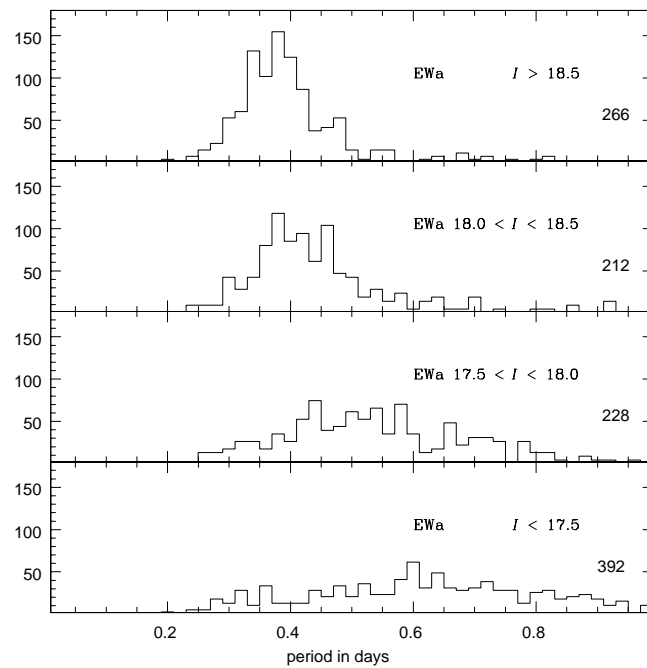


Fig. 6. Period distributions for contact binaries with unequal depths of minima in different ranges of brightness.

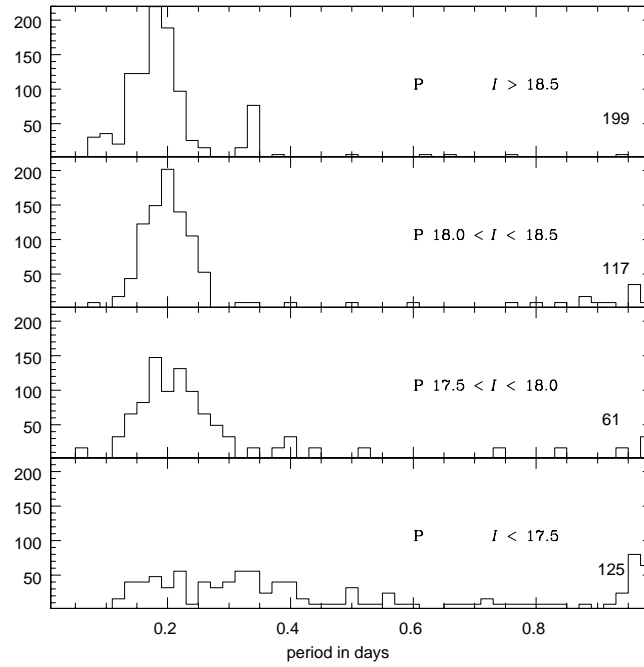


Fig. 7. Period distributions of the pulsating stars in the catalog for different ranges of brightness.

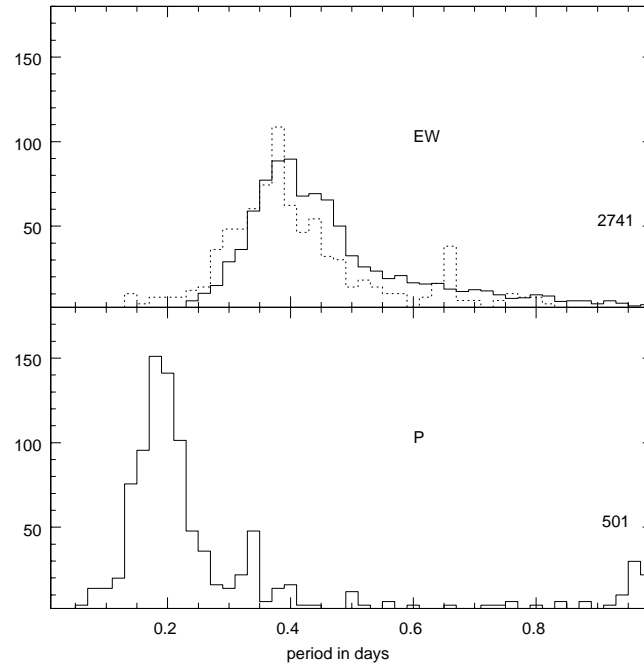


Fig. 8. Comparison of the period distribution of all contact binaries (upper panel, continuous line) with that of the pulsating variables (lower panel). Dotted line in the upper panel shows the period distribution of pulsating stars obtained with the assumption that all of them are misclassified contact binaries with periods two times longer. Histograms are normalized to 1000 objects; the true numbers of EW and P objects are given in lower right corners of both panels.

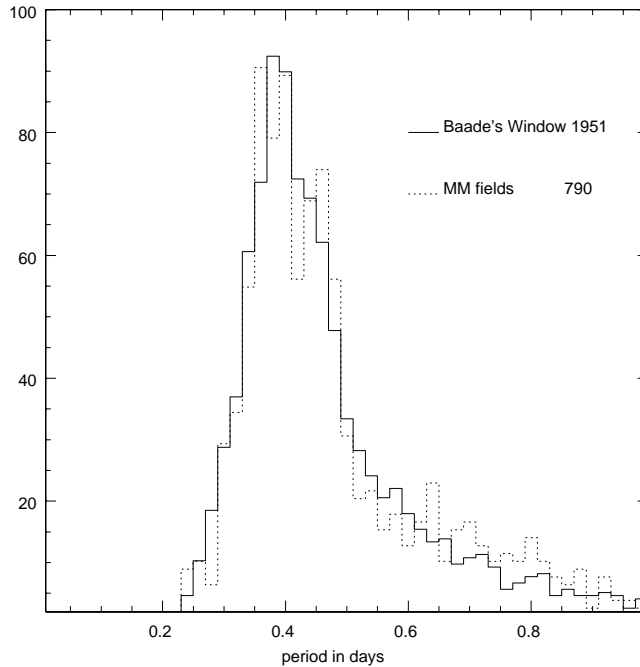


Fig. 9. Comparison of period distributions of contact binaries from the central part of the Baade’s window (continuous line) and from the MM fields in the Galactic bar (dotted line).

closer at the period distributions of the stars classified as pulsating variables. They are shown in Fig. 7 for the same brightness ranges as before. Except for the brightest stars,  $I < 17.5$  mag, all the distributions seem to be concentrated around the period 0.2 d with no obvious dependence of the maximum position on brightness. Fig. 8 compares the period distributions of all EW binaries (upper panel, continuous line) and pulsating variables (lower panel). Distributions are normalized to 1000 objects; true number of objects is also given in Fig. 8. Dotted line in the upper panel of Fig. 8 represents the period distribution of the pulsating stars from the lower panel obtained with the assumption that all of them are misclassified contact binaries with periods two times longer than pulsation periods. Both distributions look very similar suggesting that erroneous classification of pulsating stars as contact binaries affects the period distribution of contact binaries uniformly in the whole range of periods, maybe with exception of the longest periods. The small shift of the dotted histogram toward the smaller period values reflects the existence of very short periods among pulsating stars and their absence among contact binaries. Thus, the shape of the period distribution itself does not give information on the “purity” of our sample of contact binaries. We think, however, that the distinction between pulsating stars and contact binaries according to Fig. 1 is statistically acceptable.

During the first phase of the OGLE project we observed twelve field near the center of the Baade’s window and six fields in the Galactic bar (“MM” fields in Table 1). 790 contact binaries were identified in “MM” fields. Fig. 9 compares the distribution of their periods with the period distribution of contact binaries in the central part of the Baade’s window. Within the scatter limit there is no difference between these two distributions.

## 6 Period–Brightness Relation

Construction of the period–luminosity relation requires a knowledge of absolute magnitudes which are not known for our sample. We think, however, that some general features of the relation period – observed brightness suggests that we are dealing with objects the majority of which is probably located at the distance of the Galactic bulge. Fig. 10 shows this relation for contact binaries from our sample: panel (a) – for stars corrected for interstellar extinction, as described in Section 4, and panel (b) – for all stars, without correction. On both diagrams one can see a sequence defined by markedly enhanced density of points. Continuous lines in panel (a) represent the expected relation between brightness and period for contact binaries composed of two equal main sequence stars revolving in orbits with major semi-axis equal to 1.2, 1.35, and 1.5 of their radii, respectively, and located at the distance modulus 14.6 mag. The spectral type symbols mark the approximate positions of stars of these spectral type on

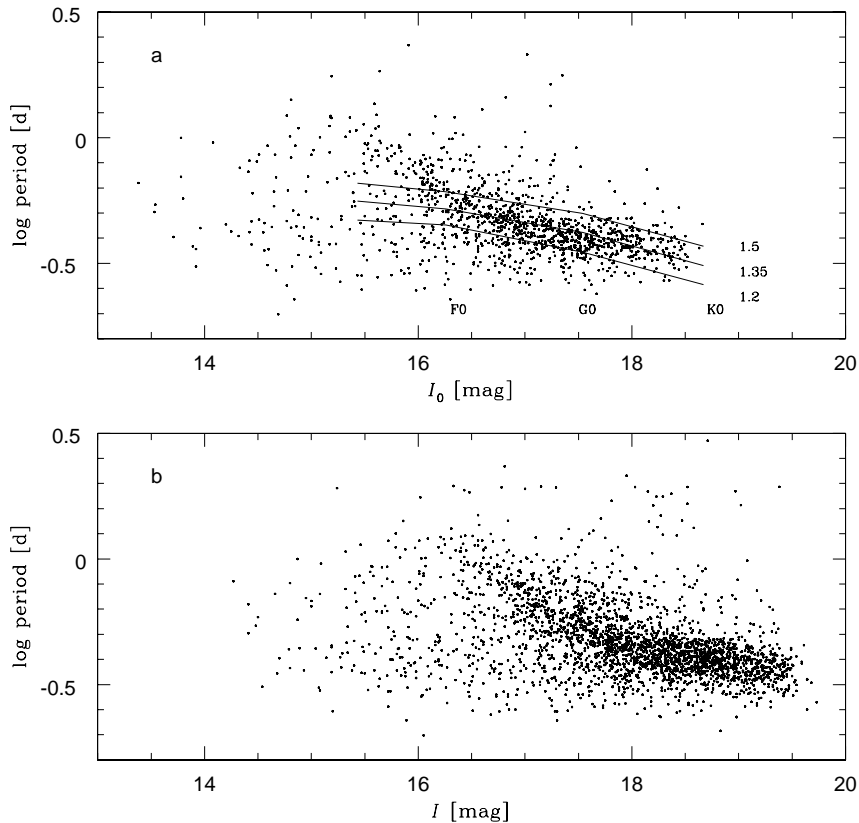


Fig. 10. Period – brightness relation for contact binaries in the present catalog. (a) – objects corrected for the interstellar extinction. Continuous lines represent the expected period – luminosity relation (shifted to fit the stars at the Galactic bulge distance) for binaries composed of two equal main sequence stars in an orbit with semi axis equal to 1.2, 1.35, and 1.5 of their radii. (b) –the same relation for all stars not corrected for the interstellar extinction.

$I_0$  brightness axis.

The existence of the relation in Fig. 10 supports our assumption that most of contact binaries from our catalog are located at the same distance, otherwise the points in Fig. 10 would be distributed much more uniformly. The shape of the relation is determined by the details of the evolution of contact systems and should be compared with expectations of particular theories. In general outlines, however, it seems to be consistent with the following simple scheme: the evolutionary not advanced objects of spectral type later than about F5 follow the period–brightness relation not very different from that for the contact main sequence stars. During their evolution, which in the plane of the figure moves a stars from right down to left up, they increased their radii not much more than by a factor of 1.5. Stars of earlier spectral types increased their radii much more, filling much bigger Roche lobes; they are responsible for bending up of the sequence in Fig. 10. The sequence is additionally broadened by differences in mass ratio: changing it from 1 towards smaller values moves the contact binary down, toward shorter periods. Thus, the faint stars with periods shorter than about 0.3 day can be interpreted as systems with particularly low mass ratio, with at least one component being a main sequence star. This scheme fits better the contact binaries with equal depths of minima, as can be seen from the Fig. 11: the relation period–brightness is much better defined for EWs than for EWa objects.

## 7 Amplitude Distribution

Amplitudes of brightness variations were determined from the decomposition of light curves into Fourier harmonics. Fig. 12 shows some examples of the observed light curves (empty symbols) and synthetic light curves obtained as the sums of five Fourier harmonics (dots), as described in Section 2.

The amplitude of light variation was determined as a difference between the brightest and the faintest points in the synthetic light-curve. Because the procedure of the Fourier decomposition into five harmonics failed in some cases, the number of objects with determined amplitudes is slightly smaller (2522) than the number of objects in the catalog.

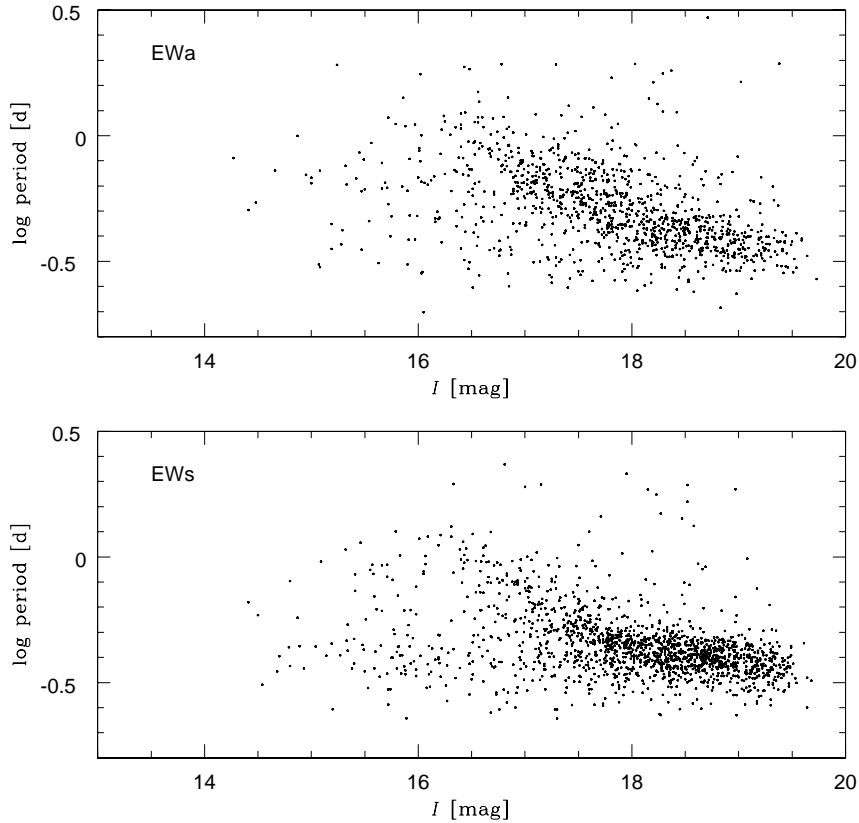


Fig. 11. Period – brightness relation for contact binaries from the present catalog, not corrected for the interstellar extinction. (a) – stars with unequal depths of minima. (b) – stars with equal depths of minima.

Distributions of thus determined amplitudes for EWs and EWa objects are given in Fig. 13. As it can easily be seen they are practically identical. This fact strongly suggests that – as it could be expected – the observed amplitude distribution of contact binaries is determined by geometrical factors rather than the physical state of the system.

In Fig. 14 we compare the distribution of amplitudes for all EW stars with that for the pulsating stars. These distributions are markedly different, in particular at small amplitudes. Amplitude distribution for pulsating stars falls down abruptly for values smaller than about 0.05 mag where observational errors become comparable with amplitudes themselves. The number of contact binaries starts diminishing less steeply and at amplitude value much bigger – about 0.2 mag. This result is rather unexpected. From purely geometrical reason the observed number of contact binaries with small amplitudes should rise monotonically as the amplitude approaches zero and only obvious selection effect makes it fall to zero at zero amplitude. Fig. 14 proves that in the case of EW-type light curves this effect starts for some reason at amplitudes much bigger than it happens in the case of pulsating variables.

## 8 Conclusions

During the first phase of OGLE project we identified 2741 objects with EW-type light curves. The majority of them belong most probably to the Galactic bulge. If it is true they constitute a sample with homogeneous population characteristics. Although all information we have about these stars is limited to the photometric features only, we think that the great number of objects in the sample allows some statistical conclusions to be drawn:

Decomposition of the EW-type light curves into Fourier harmonics provides a mean of distinguishing in a statistical way the contact binaries from pulsating variable stars.

There is no statistical difference in distributions of brightness and amplitudes of contact binaries with equal and different depths of minima. Both groups differ slightly in period distribution.

The probability of discovery of a pulsating variable star fainter than  $I = 18$  mag is in our sample at most 60%. Surprisingly, the probability of discovery of a faint contact binary is even less, what results in a severe selection effect in observed amplitude distribution.

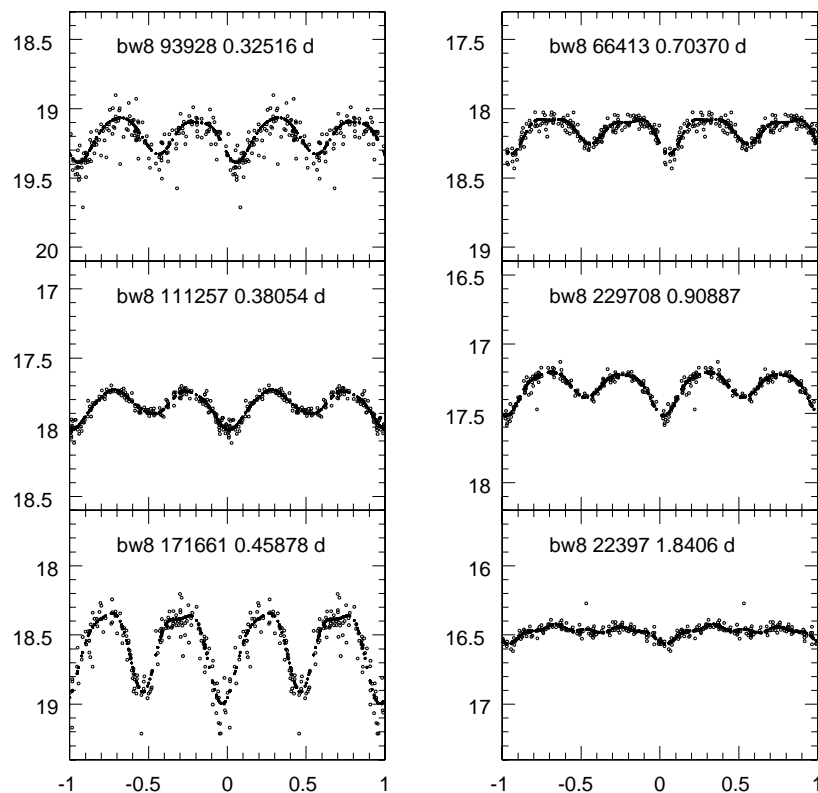


Fig. 12. Typical observed light curves (empty symbols) and the synthetic light curves obtained from the Fourier decomposition (filled symbols). Given are: the name of the field, the number in the OGLE database and the period in days.

The character of the statistical relation between period and brightness of contact binaries reflects the evolutionary state of their components. If this relation refers to objects located in the Galactic bulge then it can be treated as an “isochrone” of objects that were able to reach the present state of contact.

**Acknowledgements.** This work was supported by the KBN Grant 2P03D01418 to M. Kubiak

## REFERENCES

- Paczynski, B. 1986, *Astrophys. J.*, **304**, 1.  
 Stanek, K.Z. 1996, *Astrophys. J.*, **460**, L37.  
 Stellingwerf, R.F. 1978, *Astrophys. J.*, **224**, 953.  
 Szymański, M., and Udalski, A. 1993, *Acta Astron.*, **43**, 91.  
 Udalski, A., Szymański, M., Kałużny, J., Kubiak, M., and Mateo, M. 1992, *Acta Astron.*, **42**, 253.  
 Udalski, A., Szymański, M., Kałużny, J., Kubiak, M., and Mateo, M. 1993a, *Acta Astron.*, **43**, 69.  
 Udalski, A., Szymański, M., Kałużny, J., Kubiak, M., Krzemiński, W., Mateo, M., Preston, G.W., and Paczyński, B. 1993b, *Acta Astron.*, **43**, 289.  
 Udalski, A., Kubiak, M., Szymański, M., Kałużny, J., Mateo, M., and Krzemiński, W. 1994, *Acta Astron.*, **44**, 317.  
 Udalski, A., Szymański, M., Kałużny, J., Kubiak, M., Mateo, M., and Krzemiński, W. 1995a, *Acta Astron.*, **45**, 1.  
 Udalski, A., Olech, A., Szymański, M., Kałużny, J., Kubiak, M., Mateo, M., and Krzemiński, W. 1995b, *Acta Astron.*, **45**, 433.  
 Udalski, A., Olech, A., Szymański, M., Kałużny, J., Kubiak, M., Mateo, M., and Krzemiński, W. 1996, *Acta Astron.*, **46**, 51.  
 Udalski, A., Olech, A., Szymański, M., Kałużny, J., Kubiak, M., Mateo, M., Krzemiński, W., and Stanek, K.Z. 1997, *Acta Astron.*, **47**, 1.  
 Woźniak, P.R., and Stanek, K.Z. 1996, *Astrophys. J.*, **464**, 233.

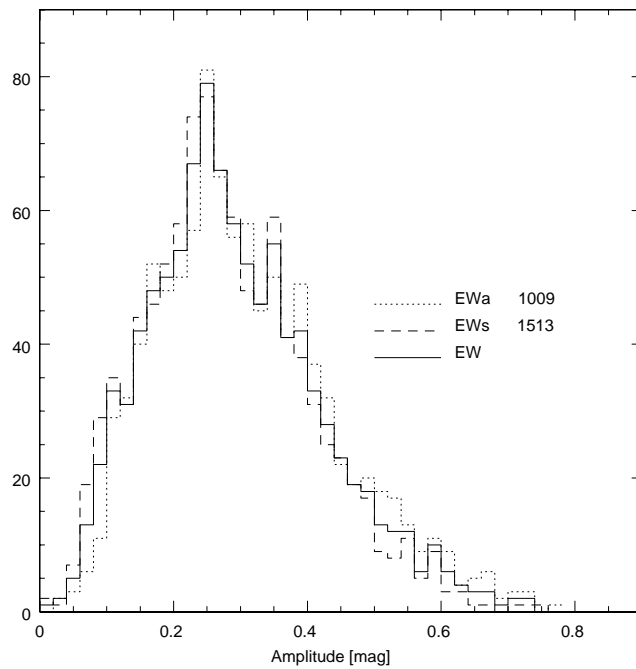


Fig. 13. Amplitude distributions for the contact binaries with equal and different depths of minima. True number of each kind of objects is given.

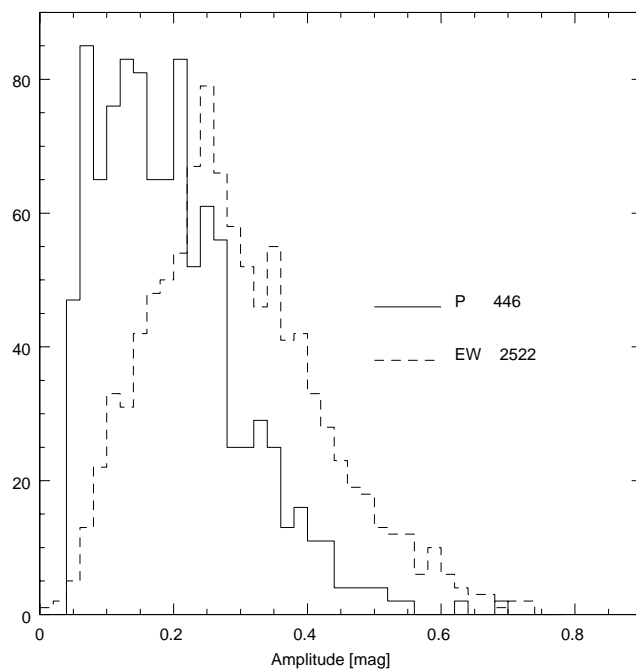


Fig. 14. Amplitude distributions for contact binaries (broken line) and for pulsating stars (continuous line) from the present catalog. True numbers of objects of both kinds are given.